

Electronic Supporting Information

A cyano-bridged single-chain magnet featuring alternate high- and low-spin manganese(III) porphyrins

Xi Chen, Shu-Qi Wu, Ai-Li Cui and Hui-Zhong Kou*

Synthesis. Sodium cyanide (19.6 mg, 0.4 mmol) was added into the solution of $[\text{MnTPP}(\text{H}_2\text{O})_2]\text{Cl}$ (73.9 mg, 0.1 mmol) in methyl cyanide. tris(2-pyridylmethyl)amine (29 mg, 0.1 mmol) and equiv manganese(II) perchlorate hexahydrate were mixed in 10 mL methyl cyanide, which was then added into the former solution. The dark green solution turned to dark brown, and was then kept in dark place for several days. Black plate-shaped crystals were collected by evaporation. IR (KBr, cm^{-1}): 2143 ($\text{C}\equiv\text{N}$). Anal. Calcd: C 77.92, H 4.07, N 10.10. Measured: C 77.8, H 4.1, N 10.2.

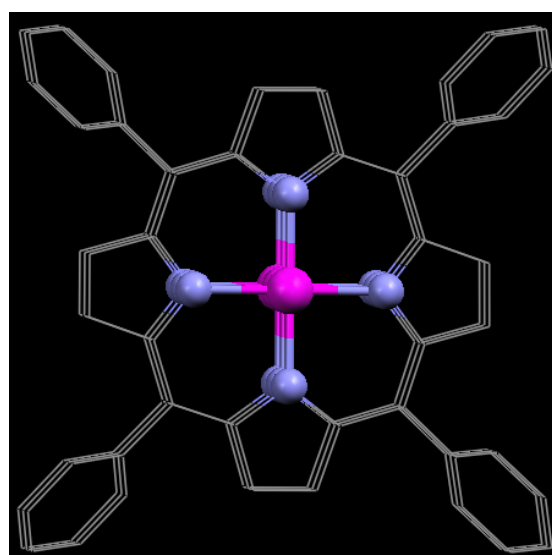


Fig. S1. Side view of the chain.

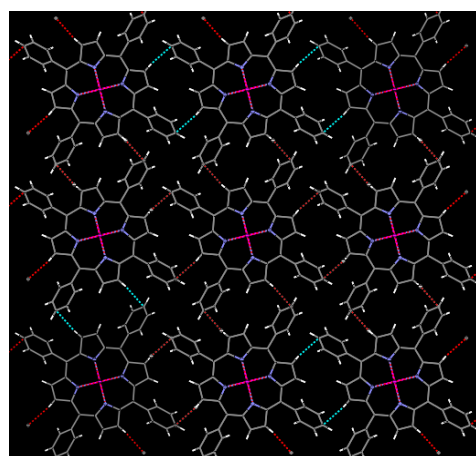


Fig. S2. The C-H--- π interactions between adjacent chains (along the *c* axis).

Fit of $\chi_m T$. An octatomic cyclic annular alternating-spin model was assumed for fitting the magnetic susceptibilities curve based on Hamiltonian. The best-fitting results are $J = +2.187 \text{ cm}^{-1}$, $g = 2.152$, when an identical J value is defined between every neighbour cores.

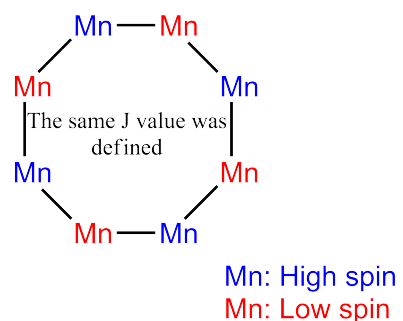


Fig S3. The octatomic cyclic annular alternating-spin model for fitting the magnetic susceptibilities.

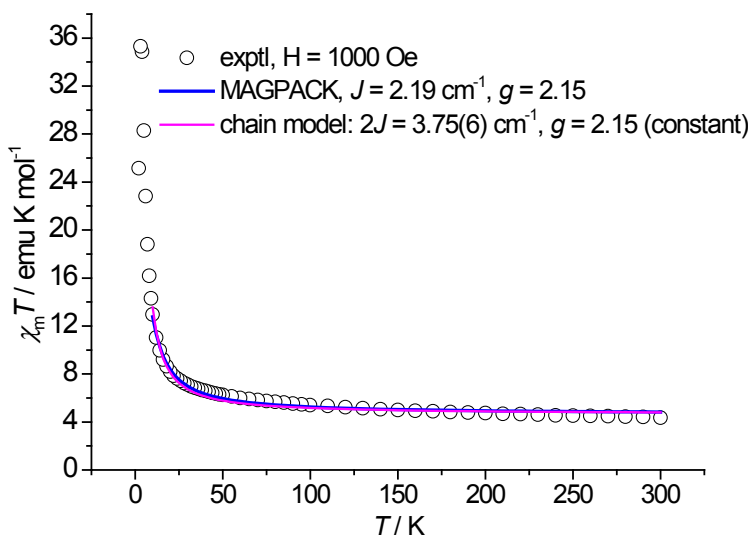


Fig S4. Comparison of the magnetic fitting results for the two models.

Fit of Cole-Cole plots. Declining-semicircle shapes were observed in the figure of Cole-Cole plots (Fig. 4), indicating the existence of double magnetic relaxations. The derivation of Debye model mentioned in the text is applied and displayed here:

$$\chi'_M = \chi_1 + (\chi_T - \chi_S) \left(\frac{\beta(1 + (\omega\tau_1)^{1-\alpha_1}) \sin\left(\frac{\pi}{2}\alpha_1\right)}{1 + 2(\omega\tau_1)^{1-\alpha_1} \sin\left(\frac{\pi}{2}\alpha_1\right) + (\omega\tau_1)^{2(1-\alpha_1)}} + \frac{(1-\beta)(1 + (\omega\tau_2)^{1-\alpha_2}) \sin\left(\frac{\pi}{2}\alpha_2\right)}{1 + 2(\omega\tau_2)^{1-\alpha_2} \sin\left(\frac{\pi}{2}\alpha_2\right) + (\omega\tau_2)^{2(1-\alpha_2)}} \right)$$

$$\chi''_M = (\chi_T - \chi_S) \left(\frac{\beta((\omega\tau_1)^{1-\alpha_1}) \cos\left(\frac{\pi}{2}\alpha_1\right)}{1 + 2(\omega\tau_1)^{1-\alpha_1} \sin\left(\frac{\pi}{2}\alpha_1\right) + (\omega\tau_1)^{2(1-\alpha_1)}} + \frac{(1-\beta)((\omega\tau_2)^{1-\alpha_2}) \cos\left(\frac{\pi}{2}\alpha_2\right)}{1 + 2(\omega\tau_2)^{1-\alpha_2} \sin\left(\frac{\pi}{2}\alpha_2\right) + (\omega\tau_2)^{2(1-\alpha_2)}} \right)$$

The formulas above were applied in the function *Nonlinear Curve Fit* of Origin 8.5. The fitting results were collected in Table S3.

Table S1. Parameters in double magnetic relaxations

Temp / K	α		τ		χ		β
	α ₁	α ₂	τ ₁	τ ₂	χ _T	χ _S	
2	0.41519	0.36547	0.00499	0.20018	6.21063	32.39551	0.19262
2.5	0.41189	0.14956	0.00166	0.03105	8.85251	23.06041	0.56491

Fit of relaxation time. The blocking temperatures in each frequency measured were chosen to constitute $\ln(1/\tau)$ vs. $1/T$ plots from $\chi''_M - T$, where $\tau = 1/(2\pi\nu)$. Based on Arrhenius relationship $1/\tau = (1/\tau_0)\exp(-\Delta_{\text{eff}}/k_B T)$, intercept and slope were used to

gain τ_0 and Δ_{eff} .

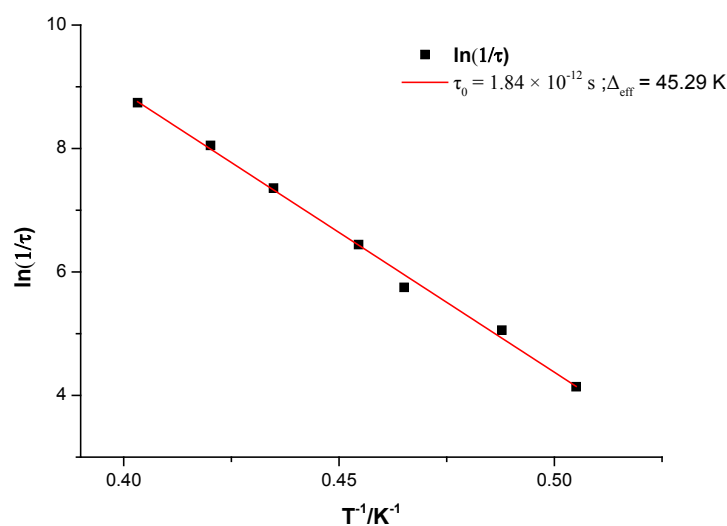


Fig S5. The $\ln(1/\tau)$ vs. $1/T$ plot based on Arrhenius relationship.

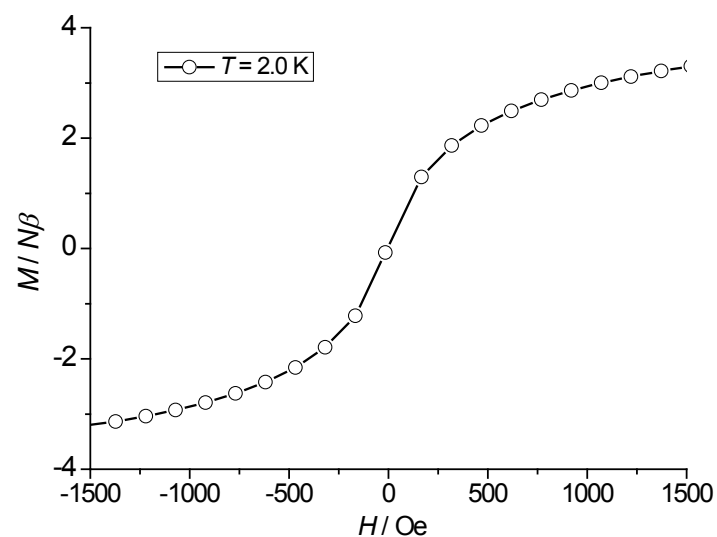


Fig S6. Field dependence of the magnetization at 2.0 K for complex **1**.